Available online at www.sciencedirect.com
SCIENCE DIRECT®
Journal of Nuclear Materials 343 (2005) 116–122
journal of nuclear materials
www.elsevier.com/locate/jnucmat

Estimation of pitting damage induced by cavitation impacts

H. Soyama [a,*], M. Futakawa [b], K. Homma [a]

[a] Department of Mechanical Engineering, Graduate School of Engineering, Tohoku University, Aoba 6-6-01, Aramaki, Aoba-ku, Sendai 980-8579, Japan
[b] Japan Atomic Energy Research Institute, Tokai-mura, Ibaraki-ken 319-1195, Japan

Abstract

In order to estimate the lifetime of the mercury target vessel of spallation neutron source which will be subjected to cavitation impacts, prediction methods of pitting damage induced by the cavitation impact were proposed. It is very important to estimate the incubation time, in which plastic deformation occurs without mass loss, because the thickness of the vessel is very small. In the present paper, two estimation methods were proposed. One of them is the estimation from erosion tests of severely damaged specimens by plotting the mass loss as a function of exposure time to cavitation on the logarithmic scales. Another method is the observation of plastic deformation pits on damaged surfaces at very early stages during incubation.

1. Introduction

The Japan Atomic Energy Research Institute (JAERI) and the High-Energy Accelerator Research Organization (KEK) are cooperatively constructing a new MW-scale spallation neutron source for new science fields such as material and life science in a joint project, i.e., Japan Proton Accelerator Research Complex (J-PARC) [1]. JAERI and KEK are going to use liquid-mercury as the target and coolant in J-PARC. A similar system is also being constructed at Oak Ridge National Laboratory (ORNL). Futakawa et al. observed pitting damage induced by cavitation in mercury through off-line tests related with pressure wave propagation [2,3] and after words by ORNL in the on-beam test using the proton beam at Los Alamos Neutron Science Center (LANSCE) [4]. As the thickness of target vessel is very small, it is very important to estimate the pitting damage as a decisive issue for the structural integrity of target.

In the case of the MW-scale spallation neutron source system in J-PARC, the proton pulsed beam with 1 μm pulse-width will be injected into the mercury through the beam window of the target vessel at a frequency of 25 Hz [3]. The proton beam injection produces a thermal shock in the mercury and the released pressure wave propagates to the vessel wall, where it causes cavitation which leads to pitting damage [5,6].

Normally, the progress of cavitation erosion is classified into: incubation stage, acceleration stage, maximum rate stage and deceleration stage [7,8]. In the incubation stage, plastic deformation occurs on the material surface without mass loss. When the exposure time to cavitation is long enough, the mass loss starts and the mass loss rate increases with erosion time. Thus it is called the acceleration stage. When mass loss rate has reached to constant value, which is normally maximum through the all stages, it is called the maximum rate stage. In

* Corresponding author. Tel.: +81 22 217 6891; fax: +81 22 217 3758.
E-mail address: soyama@mm.mech.tohoku.ac.jp (H. Soyama).

0022-3115/$ - see front matter © 2005 Elsevier B.V. All rights reserved.
doi:10.1016/j.jnucmat.2004.11.016

the maximum rate stage, the erosion rate is constant for a while, thus the maximum rate stage is also called steady state stage. Here, the nominal incubation time is also defined by the intercept point of the maximum erosion rate line on the time axis. In order to estimate the nominal incubation time, a precise erosion test is required. As the ratio of erosion rate of different materials depends on the cavitation loading [9], the erosion rate should be measured at on-beam test. However, many points cannot be obtained by the on-beam test. Therefore, a method to estimate the incubation period from a few points is required.

Futakawa et al. found that the normalized MDE (mean depth erosion) is adequately plotted on the homologous line given by the following equation by using the data of vibratory horns and magnetic impact testing [10]:

$$\mathrm{Log}\,\mathrm{MDE} = A\,\mathrm{Log}N + B, \tag{1}$$

where $A = 1.3$, $B = f$(materials, temperature, pressure, etc.) and N is the number of cycles. The constant of B related with the incubation period is strongly dependent on the material, liquid temperature and imposed pressure, while the A value is independent of materials and cavitation intensity [10]. That is, the MDE in the steady state is predicted by Eq. (1). Based on this equation, furthermore, Soyama and Futakawa proposed an estimation method of the incubation time by plotting the mass loss as a function of exposure time to cavitation on the logarithmic scales [11]. However, the reason for A to equal 1.3 is not clear in our previous paper. In order to generalize the method, one of the reasons is discussed.

Futakawa et al. found that the mass loss starts when plastic deformation pits covered nearly the entire area, i.e., 98% coverage [12]. Here the coverage is defined by the ratio of plastic deformation pit area to total area. Thus, if the coverage changing with exposure time to cavitation is clarified, the incubation time will be estimated by observing the damaged surface at a very early stage.

In the present paper, in order to predict the lifetime of the target vessel of the spallation neutron source, two methods to estimate the incubation time are proposed. One of them analyzes the erosion curve by plotting the mass loss as a function of exposure time to cavitation on the logarithmic scales. This method requires steady state erosion. The erosion data from a cavitating jet apparatus in accordance with ASTM G-134-95 [7] for various materials and different conditions was discussed to reveal the reliability of the proposed estimation method. The advantage of the proposed method is to estimate sufficiently the incubation time from one point of mass loss data in the steady state, although the incubation time is normally estimated from an erosion curve with points. Another method is to estimate the incubation time from the observation of coverage of pitting due to plastic deformation at a very early stage. In order to estimate the incubation time from the coverage, the numerical simulation of coverage was carried out to find the unique locus line that reveals the coverage of pitting due to plastic deformation changing with time.

2. Experimental facilities and procedures for erosion test

Fig. 1 illustrates a cavitating jet apparatus in accordance with ASTM G-134-95 [7] for cavitation erosion tests. Water was injected into the water-filled test section through a nozzle by a plunger pump. The nozzle diameter was 0.4 mm and the discharge coefficient of the nozzle was 0.64. The cavitation intensity of the jet can be changed by adjusting the injection pressure p_1 of cavitating jet and the tank pressure p_2 [7,13]. The optimum standoff distance s for the erosion test varied with p_1 and p_2 [7,13]. The test conditions were as follows: (i) $p_1 = 15$ MPa, $p_2 = 0.21$ MPa, $s = 19$ mm, (ii) $p_1 = 20$ MPa, $p_2 = 0.28$ MPa, $s = 19$ mm, (iii) $p_1 = 20$ MPa, $p_2 = 0.5$ MPa, $s = 14$ mm, (iv) $p_1 = 30$ MPa, $p_2 = 0.42$ MPa, $s = 19$ mm. Deionised water was used in the cavitating jet loop. The details of the erosion test may be found in Ref. [13].

The materials tested were pure aluminum (Japanese Industrial Standard JIS A1050), pure copper (JIS C1100), bronze casting (JIS CAC402), aluminum copper alloy (JIS CAC702), iron casting (JIS FC250), stainless steel casting (JIS SCS1, SCS13), stainless steel (JIS SUS304, SUS316, SUS316L), carbon steel (JIS S45C), general steel (JIS SS400), machinable ceramic (MACERiTE™ HSP), acrylic resin and dicyclopentadien resin (DCPD).

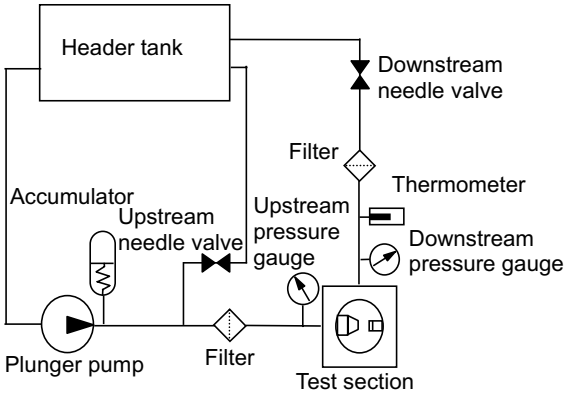

Fig. 1. Cavitating jet apparatus for erosion test.

3. Method of numerical simulation for coverage

Numerical simulations were carried out to quantitatively understand the increase of the plastically deformed area with exposure time to cavitation. The algorithm of numerical simulation is shown in Fig. 2. The simulated area was divided into small squares of assemblies of squares which show pits were randomly generated one by one. The position (x_i, y_i) of pits i was generated by using a random function as shown in Fig. 3. The shape of a pit was determined by an assembly of squares. The size of the pit is given by the number of corresponding squares. In Fig. 3, the size of pit i is 4. The size is defined by a random function, which yields a normal distribution, to consider a distribution of frequency of pits as a function of pit size. Then ratio of number of squares, where pits were generated at least once (gray region) to the total number of squares in simulated area is the corresponding coverage. The coverage was investigated as a function of the number of generated pits, which corresponds to the exposure time to cavitation impacts denoted by the number i_{max}.

In order to find a reasonable parameter to simulate the coverage numerically, the cavitation impact force and pits size were measured by using a cavitating jet in air to create a large plastic deformation pit. This means that the cavitating jet is directly injected into air without

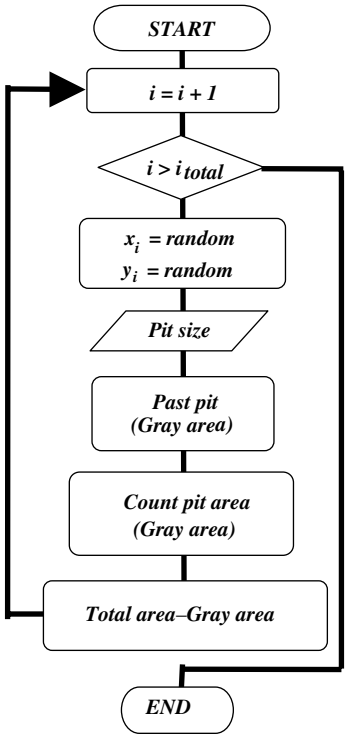

Fig. 2. Flow chart of numerical simulation of coverage.

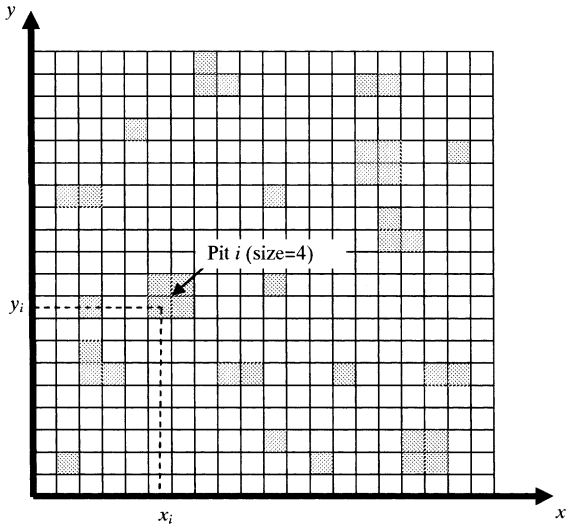

Fig. 3. Simulated area and the pits.

a water-filled chamber by injecting a high-speed water jet into a low-speed water jet, which is directly injected into air, using a concentric nozzle [14]. The nozzle diameter and the injection pressure of a high-speed water jet were 1 mm and 20 MPa, and 30 mm and 0.21 MPa for the low-speed water jet, respectively. The standoff distance was 50 mm. Table 1 shows the diameters of the plastic deformation pits on various materials. Fig. 4 shows the frequency of cavitation impacts changing with the impact force at the conditions mentioned above as measured by a custom-made transducer developed by Soyama et al. [15]. A piezoelectric polymer vinylidene fluoride (PVDF) film was used as the sensitive material. The transducer was calibrated by the pencil-lead breaking method. The details of the transducer and the calibration method are as in Ref. [15].

The distribution of pit size and frequency was assumed as same as that of the impact size and the frequency of impact in the present paper, as large pits were produced by large impact force. The fundamental threshold level of cavitation impact, which means that the impacts larger than the threshold level produce plastic deformation, is about 80 N [13]. In Fig. 4, small impacts take place frequently and the number of large

Table 1
Pit diameter

	Pit diameter, d (μm)
Fe	59.2 (7.3)
Cu	136.2 (37.9)
Al	230.0 (82.6)
Pb	568.2 (198.0)

The value in brackets show standard deviation.

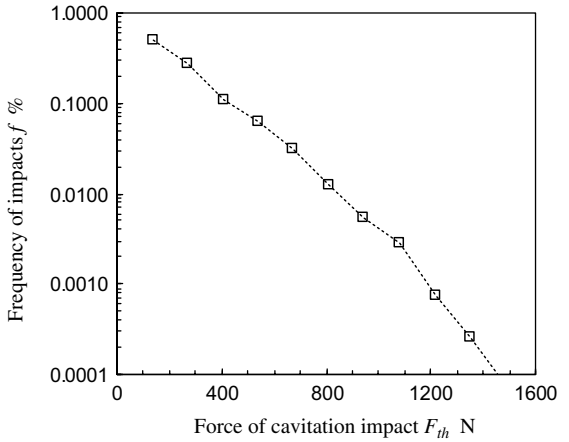

Fig. 4. Relation between force of cavitation impact and frequency of impacts.

impacts is considerably small. Large impacts whose size was 15 times larger than 80 N, were produced. The smallest size of pits will be several tens micro-meter as shown in Table 1. In the present paper, smallest size of simulated pits was assumed as 30 μm × 30 μm and the largest pits to be 15 times larger than smallest ones. The simulated area consists of squares of 500 × 500, which corresponds to the actual size of 15 mm × 15 mm. The total number of pits in this simulation is 1 000 000 corresponding to 100% coverage.

4. Results

4.1. Estimation of incubation time from erosion test

Our proposed method based on the relation between the mass loss $\Delta m = 1$ mg and the cavitation exposure time t can be described by the following equation:

$$\mathrm{Log}\,\Delta m = A\,\mathrm{Log}\,t + B, \tag{2}$$

where A and B are constants, the value of constant A is 1.3 for water [11]. The constant B corresponds to the incubation time. When the intercept of mass loss line on $\Delta m = 1$ mg for the convenience, the incubation time in minutes is estimated by plotting the mass loss as a function of exposure time to cavitation on the logarithmic scales. One point is enough for the estimation, although several points would be preferred for increased accuracy.

Fig. 5 illustrates the mass loss as a function of cavitation exposure time, (a) for various materials at $p_1 = 20$ MPa, $p_2 = 0.28$ MPa, and (b) with several cavitating conditions for stainless steel JIS SUS316. For all the cases, the mass loss Δm was scarcely at early stages, i.e., incubation stages, and gradually increased at acceleration stage, then the mass loss curve shows straight line at steady state stage, finally the slope of mass loss vs. time was decreased at deceleration stage. When the relations between the mass loss and the exposure time were plotted on a log–log scale, the slope n was 1.3 for all materials and cavitating conditions [11]. Thus the incubation time can, in fact, be estimated from quantitative measurements of the erosion rate at a point after incubation.

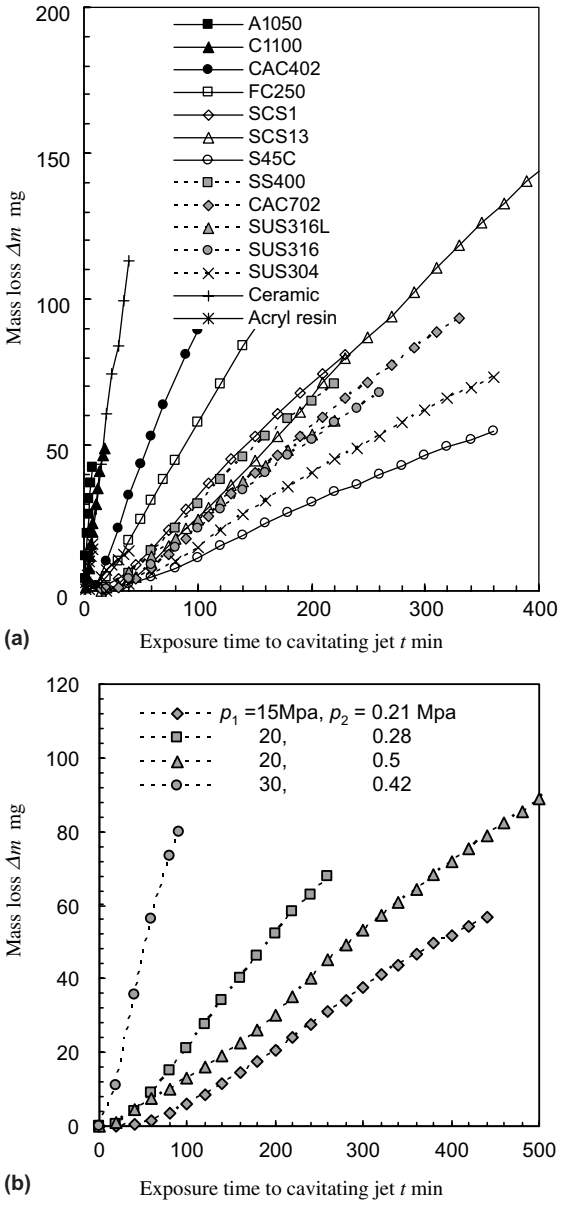

Fig. 5. Mass loss with time for (a) various materials ($p_1 = 20$ MPa, $p_2 = 0.28$ MPa); (b) several cavitating conditions (stainless steel JIS SUS316).

Additionally, in order to investigate the reason of $n = 1.3$, the exposure time t and the mass loss Δm of the all data in Fig. 5 were normalized by the exposure time t_{max} and the mass loss Δm_{max} to reach the maximum erosion rate, respectively as follows:

$$\overline{\Delta m} = \Delta m / \Delta m_{max}, \tag{3}$$

$$\bar{t} = t / t_{max}. \tag{4}$$

All the data are plotted in Fig. 6, to yield the same line. This means that, when the normalized, each stage such as incubation, acceleration, steady state and deceleration exhibit the same trend independently of materials and cavitation conditions. Namely, the ratio of incubation time to the time to reach the maximum erosion rate is constant. Furthermore, the normalized mass loss of each stage is also nearly constant for all cases. The unique line is approximated as follows:

$$\overline{\Delta m} = c_1\bar{t} + c_2\bar{t}^2 + c_3\bar{t}^3 + c_4\bar{t}^4 + c_5\bar{t}^5. \tag{5}$$

Here, c_1, c_2, c_3, c_4 and c_5 are constants, and $c_1 = -0.0003$, $c_2 = 2.9783$, $c_3 = -3.2157$, $c_4 = 1.4941$ and $c_5 = -0.258$, respectively.

Fig. 7 shows the fifth order as the polynomial approximation described in Eq. (4) on a log–log scale. The post of the curve describing the steady state is represented by solid line. Here, points before and after the maximum erosion rate stage, whose mass loss rate is larger than 80% of maximum mass loss rate, are assumed to be the steady state stage. Stages before and after the steady state are described by dotted lines. The slope of the solid line is nearly 1.3. This value coincides with the results for mercury [10,12] and water [11].

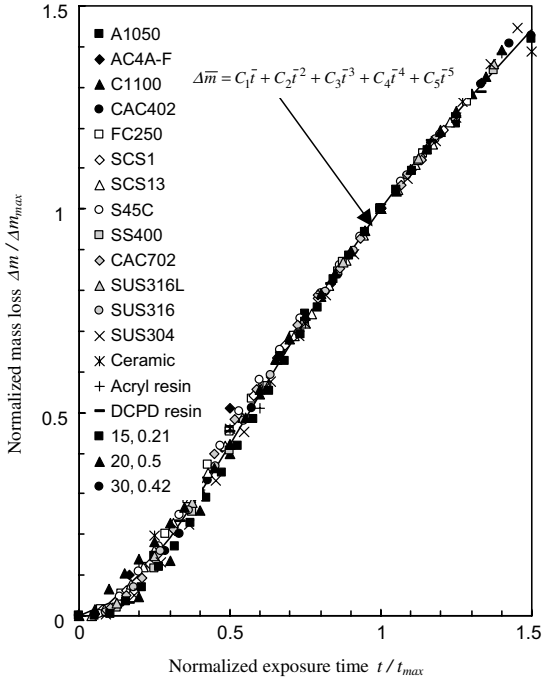

Fig. 6. Normalized mass loss curve.

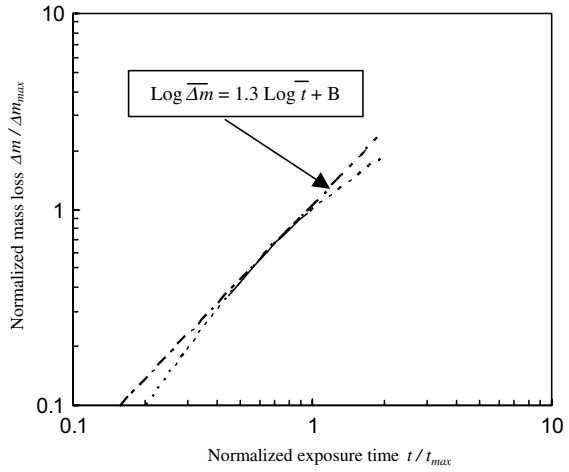

Fig. 7. Approximation line on a log–log scale.

4.2. Coverage as a function of exposure time to cavitation impact

Fig. 8 shows the relationship between the size and the frequency of the pits. The frequency was normalized by the total number of the generated pits. The normal distribution is also shown in Fig. 8 as a solid line. Generated 1 000 000 pits are normally distributed. The maximum size of generated pits is 15 times larger than that of smallest pits, which corresponds to 30 μm × 30 μm. The range of size will be reasonable because of above mentioned distribution of cavitation impact in Fig. 4.

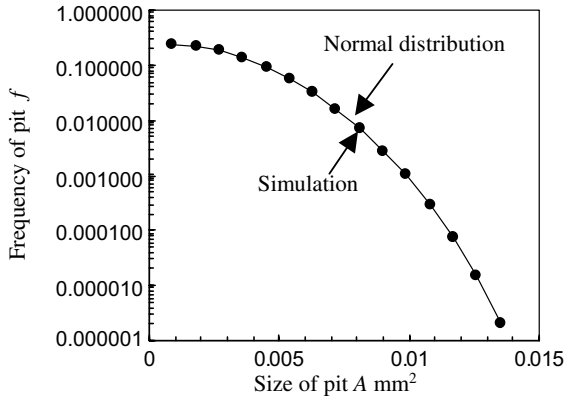

Fig. 8. Size distribution of generated pits.

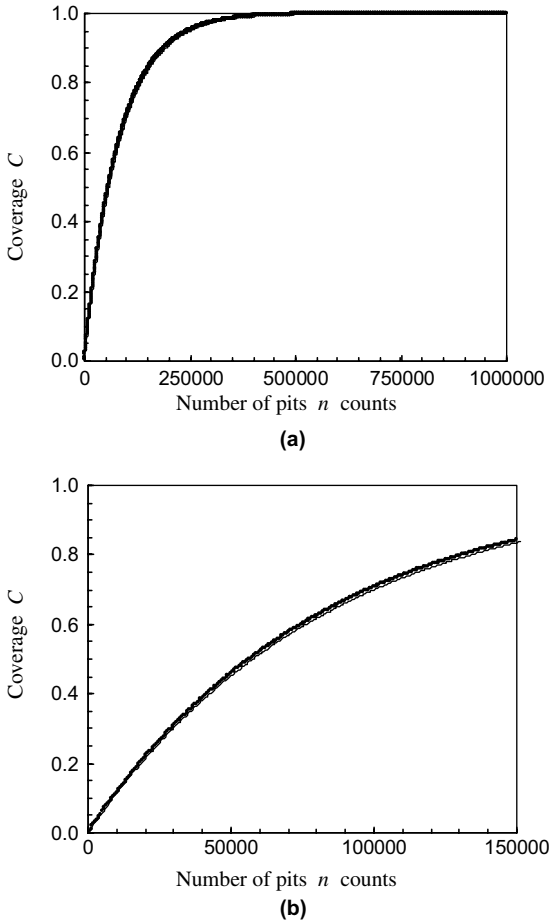

Fig. 9. Coverage as a function of number of pit. (a) $0 \leqq n \leqq 1\,000\,000$ and (b) $0 \leqq n \leqq 150\,000$.

Fig. 9 illustrates the coverage as a function of the number of pits. As the pits are generated one by one, the number of pit reveals a kind of exposure time to cavitation impact. Fig. 9(a) shows the number of pits $0 \leqq n \leqq 1\,000\,000$ and Fig. 9(b) shows the number of pits $0 \leqq n \leqq 150\,000$ to magnify the early stage of erosion time. Practically the pits do not overlap at $0 \leqq n \leqq 20\,000$, the coverage increases linearly with the number of pits. The rate of increase decreases after $n = 20\,000$, and saturates. The following equation for coverage C was assumed with the reference to the results of coverage on shot peening.

$$C = 1 - e^{an}. \tag{6}$$

Here, a is constant. The constant $a = -1.2 \times 10^{-5}$ was obtained from the coverage C and the number n at $C = 0.5$. The curve of Eq. (5) for $a = -1.2 \times 10^{-5}$ is shown in Fig. 9, and agrees well with the results of numerical simulation cavitation. Thus, it can be concluded that the coverage C as a function of exposure time t is described by the following equation:

$$C = 1 - e^{at}. \tag{7}$$

The constant a will be obtained by the measurement of coverage at some time. When the coverage at least one time was obtained to know the constant a, the coverage at any time can be obtained by using Eq. (7). The experimental coverage of plastic deformation measured by a laser profilometer as a function of the exposure time to cavitation impact was correlated by Eq. (7) for various materials and different cavitating conditions [12]. In the results of paper [12], the incubation time was defined as the time of 98% coverage.

5. Discussions

Two different methods were proposed to estimate the incubation time in the present paper. The schematic

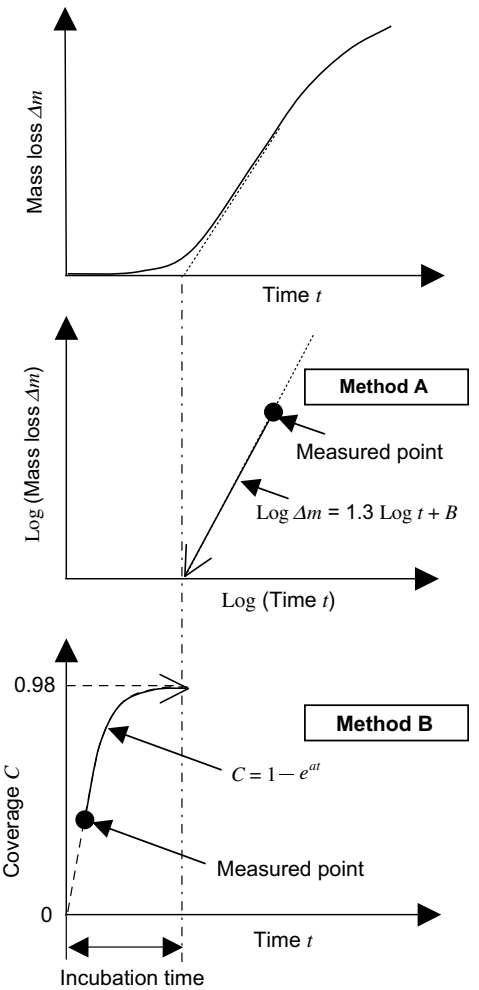

Fig. 10. Schematic diagram of estimation of incubation time by method A and B.

diagram to estimate the incubation period was shown in Fig. 10. Method A uses the erosion data after the incubation stage. Although the mass loss was used for the quantity of cavitation erosion in the present paper, the mean depth of erosion is also useful to evaluate cavitation erosion [12]. Method B is based on observation of the coverage on the surface at an early stage of incubation period. The sequential step of the methods are as follows:

A. 1. Measure the mass loss Δm or mean depth of erosion MDE to obtain the constant B in Eqs. (1) or (2). At least one point is required.
   2. Plot the mass loss Δm or mean depth of erosion MDE versus time on a log–log scale.
   3. Draw the straight line at an inclination 1.3 on the above figure.
   4. Obtain the incubation time in minutes from the intercept of above straight line with the time axis at $\Delta m = 1$ mg or MDE = 1 μm.

B. 1. Measure the coverage at early stage in incubation period.
   2. Obtain the constant a in Eq. (7).
   3. Obtain the incubation time from the Eq. (7) at $C = 0.98$, i.e., 98%.

For both of these methods several points are suggested to increase accuracy. The cavitating condition of above mentioned tests should be the same as that of the estimated one. Of course, material was changed, the erosion test or measurement of coverage was required for both methods A and B.

6. Conclusions

In order to estimate the lifetime of a target vessel of MW-scale spallation neutron source, two experimental methods were proposed to predict the incubation time due to cavitation erosion. One of them is the estimation from erosion results of severely damaged specimen with mass loss. Another method is the observation of coverage due to plastic deformation pits at an early stage in incubation stage. Each method was generalized by the erosion test using various materials at different cavitating conditions and by numerical simulation, respectively. The main results are summarized as follows:

1. A method for the prediction of incubation time by inspection of erosion vs time, plotted on a log–log scale was proposed and generalized. The incubation time can be estimated from a point of quantitative measurements of erosion rate of severely damaged specimen.
2. Another method based on the coverage at a certain point in the early incubation stage was proposed to estimate the incubation time.

Acknowledgment

This work was partly supported by Japan Society for the Promotion of Science under Grant-in-Aid for Scientific Research (B)(2) 13555022 and 14350049.

References

[1] Planning Division for Neutron Science, in: Proceedings of 3rd Workshop on Neutron Science Project, JAERI-Conference 99-003, Tokai, 1999.
[2] M. Futakawa, H. Kogawa, R. Hino, J. Phys. IV France 10 (Pr9) (2000) 237.
[3] M. Futakawa, H. Kogawa, R. Hino, H. Date, H. Takeishi, Int. J. Impact Eng. 28 (2) (2003) 123.
[4] B. Riemer, in: Proceedings of 3rd International WS on mercury target development, ORNL, November 2001.
[5] J.R. Haines, K. Farrell, J.D. Hunn, D.C. Lousteau, L.K. Mansur, T.J. McManamy, S.J. Pawel, B.W. Riemer, SNS-101060100-TR0004 (2002) 1.
[6] S. Ishikura, H. Kogawa, M. Futakawa, K. Kikuchi, R. Hino, C. Arakawa, J. Nucl. Mater. 318 (2003) 113.
[7] ASTM Designation G-134-95, American Society for Testing and Materials (1997) 1.
[8] ASTM Designation G-32-98, American Society for Testing and Materials (2001) 1.
[9] J. Steller, Wear 233–235 (1999) 51.
[10] M. Futakawa, T. Naoe, H. Kogawa, C.C. Tsai, Y. Ikeda, J. Nucl. Sci. Technol. 40 (11) (2003) 895.
[11] H. Soyama, M. Futakawa, Tribol. Lett. 17 (1) (2004) 27.
[12] M. Futakawa, T. Naoe, C.C. Tsai, H. Kogawa, S. Ishikura, Y. Ikeda, H. Soyama, H. Date, in: Proceedings of 5th International Symposium on Cavitation, Osaka, November 2003, CD-ROM.
[13] H. Soyama, H. Kumano, J. Test. Eval. 30 (5) (2002) 421.
[14] H. Soyama, J. Eng. Mater. Technol. Trans. ASME 126 (1) (2004) 123.
[15] H. Soyama, A. Lichtarowicz, T. Momma, E.J. Williams, J. Fluids Eng. Trans. ASME 120 (4) (1998) 712.